Determining Atom-Centered Monopoles from Molecular Electrostatic Potentials. The Need for High Sampling Density in Formamide Conformational Analysis

Curt M. Breneman* and Kenneth B. Wiberg

Yale University Department of Chemisty, New Haven, Connecticut 06511

Received 12 June 1989; accepted 12 October 1989

An improved method for computing potential-derived charges is described which is based upon the CHELP program available from QCPE.[1] This approach (CHELPG) is shown to be considerably less dependent upon molecular orientation than the original CHELP program. In the second part of this work, the CHELPG point selection algorithm was used to analyze the changes in the potential-derived charges in formamide during rotation about the C—N bond. In order to achieve a level of rotational invariance less than 10% of the magnitude of the electronic effects studied, an equally-spaced array of points 0.3 Å apart was required. Points found to be greater than 2.8 Å from any nucleus were eliminated, along with all points contained within the defined VDW distances from each of the atoms. The results are compared to those obtained by using CHELP. Even when large numbers of points (ca. 3000) were sampled using the CHELP selection routine, the results did not indicate a satisfactory level of rotational invariance. On the basis of these results, the original CHELP program was found to be inadequate for analyzing internal rotations.

INTRODUCTION

The electrostatic potential field surrounding a molecule has been shown to be an important indicator of the way in which it interacts with the outside world.[2] Fortunately, the electrostatic potential is an exact one-electron property which can be readily calculated at any point in space from a molecular wavefunction. Since electrostatic interactions account for a major portion of the intermolecular forces between two molecules, they are essential in molecular mechanics and dynamics calculations.[3] These electrostatic interactions can be expressed in terms of multipole expansions. In the interest of speed, truncated expansions must be employed, and simple atom-centered monopole models are often used.[3] The monopole model has the advantage that it provides an intuitive way to think about the charge distribution within a molecule which can be compared to the results of other, more rigorous techniques.

Several methods for calculating point-charge models from *ab-initio* wavefunctions have recently appeared in the literature.[1,5-9] Both Williams[8] and Cox and Williams[9] have described methods which use regular grids of points in their fitting procedures, while Kollman and Singh[7] and Chirlian and Francl[1] (CHELP) use point selection routines which are based upon atom-centered shells of points. Kollman's program uses the Connolly molecular surface algorithm[10] to define points on several concentric shells surrounding the molecule, whereas the CHELP routine chooses 14 points for each shell ($\pm x$, $\pm y$, $\pm z$, and in the center of each octant). The public version of the CHELP program has a built-in 1.0 Å increment between concentric shells. All of the routines use approximately 200–400 points in each fit, with point spacings of 0.8–1.0 Å. Since the electrostatic potential is not well defined by a point charge model inside the molecular VDW radius, all of the fitting routines exclude these points from consideration. When each of these methods are used with appropriate wavefunctions, they yield "atomic charges" which reproduce certain molecular properties such as the dipole moment reasonably well.[1,8] During the course of this investigation, however, we found that rotational invariance problems render methods such as CHELP inappropriate for use in conformational analysis.

Our investigation revealed that the rotational variance inherent in CHELP arises from two sources: (1) The sparse point sampling, and (2) the dependence upon the molecular coordinate system for choosing test points. Analysis of the data given in the tables below suggests that

*Present Address: Department of Chemistry, Rensselaer Polytechnic Institute, Troy, New York 12181. Author to whom all correspondence should be addressed.

CCC 0192-8651/90/030361-13$04.00

the rotational dependence is more sensitive to the nature of the point selection routine than to the actual number of points utilized. The original QCPE CHELP results did not change significantly when an order of magnitude more points were used, but the resolution of the CHELPG calculations increased linearly with the number of points selected. This was found to be partially due to the fact that the built-in 1.0 Å shell increment in the public CHELP program caused the additional points to be too far away from the molecule to add any information to the fit. Consequently, in order to compare the CHELP and CHELPG methods in a fair manner, the shell increment in CHELP was changed to 0.1 Å for the runs using a large number (ca. 3000) of data points. Even with this advantage, the CHELP point charges were found to change significantly with molecular orientation. These orientational dependency problems were found to be magnified when internal rotations are being examined, since the locations of the sample points change relative to the molecule at the same time that some points are masked out by VDW constraints. In this paper, the orientational problem is examined for both inter and intramolecular motions.

THE CHELP METHOD

In this investigation, the results of CHELP calculations are compared with those of the grid-oriented CHELPG procedure. The original CHELP program[1] employs a Lagrange multiplier method to fit atom-centered point charges to a molecular electrostatic potential field. The Lagrange multiplier technique has the advantage of being fast and noniterative, so this least-squares method was retained in the CHELPG program. As in the CHELP program, only the total charge on the molecule is constrained in fitting procedure. The principal difference between the CHELPG method and the older CHELP program is that the CHELPG procedure employs a point-selection algorithm based upon regularly spaced points.

We have found that the original point selection algorithm used in the CHELP program gives results that are not invariant to either molecular coordinate system rotation, or to internal bond rotations. As a result of this random variation, CHELP analysis of internal rotation pathways is severely limited. Significant changes in the calculated point charges are also seen when the molecule is simply reoriented in the coordinate system. In this work, a point selection algorithm similar to that employed by Cox and Williams[9] was used which dramatically reduces these orientational dependencies. The algorithm involves defining a cube of points spaced 0.3–0.8 Å apart containing the molecule and including 2.8 Å of headspace on all sides. As in the original CHELP program, all points which fall inside a predefined VDW radius of any of the nuclei are discarded. In this work, two sets of VDW radii were utilized, and the results compared. All points outside the 2.8 Å maximum radius are also eliminated from the fitting procedure. The remaining points form a relatively homogeneous layer around the molecule, where all regions outside the molecular VDW radius (and within the defined interaction distance) are equally represented. Following the point selection procedure, the electrostatic potential at each of the sample points is calculated analytically from the wavefunction and geometry data contained in the Gaussian 88/90 checkpoint (.CHK) or read-write (.RWF) files. These data are then used as input for the Lagrange multiplier least-squares routine, which has been constrained to fit the exact molecular charge, but not to the molecular dipole moment. The computed best-fit charges reproduce the RHF molecular dipole moments reasonably well, as indicated in Tables III, IV, VII, and VIII.

For the formamide rotomers used in this comparison, the CHELP method selected about 350–400 points, while the high-density CHELPG typically utilized 5000–6000 points. With this density of sampling, we found that features of the molecular electrostatic potential can be smoothly quantified throughout internal rotations. As shown below in Tables IIIa, IVa, VIIa, and VIIIa, CHELPG calculations using only 250-300 points produced rotational invariances significantly better than CHELP calculations using from 400–3000 points in all cases studied. The Gaussian 88/90 compatible version of the CHELPG program has been submitted to QCPE.

RESULTS AND DISCUSSION

In connection with our continuing interest in "resonance" phenomena, a series of formamide structures were examined using both CHELP and the new CHELPG routine. In the first part of this study, the rotational dependencies of these two methods were compared by using each of them to calculate at set of "atomic charges" for the planar minimum (**1**) and *syn* rotational transition state (**2**) of formamide oriented in various positions within their respective molecular coordinate systems. The results of these calculations are shown in Tables I–VIII, where the odd-numbered tables contain data obtained using "small" VDW exclusion radii (C = 1.5 Å, N,O = 1.7 Å, H = 1.45 Å), and the even-numbered tables contain results obtained using larger exclusion radii (C, N, O = 2.0 Å, H = 1.5 Å).[11] In each of the ta-

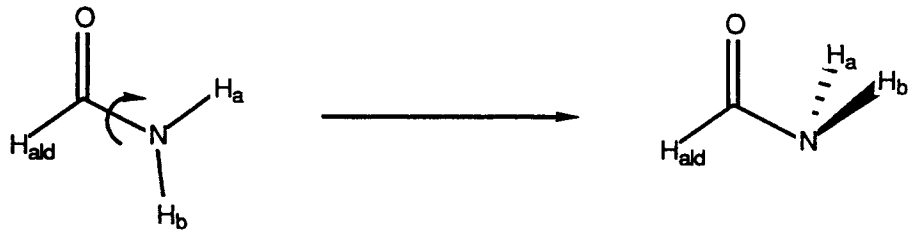

1 2

bles, the structure labeled "normal" refers to orientation in which the C-N bond is along the X-axis, and the heavy atoms are in the XZ plane. The other orientations were produced by translating the carbonyl carbon to the origin, and then rotating the indicated amount about the specified axis.

Tables I and II show the "atomic charges" for transition structure **2** calculated by CHELP with both small and large exclusion radii. Using small exclusion radii, the average nitrogen charge was calculated to be −1.0836, while the carbon and oxygen charges were calculated to be 0.8813 and −0.5941, respectively (Table I). The aldehyde hydrogen charge averages out to be slightly negative, while the amino-hydrogen charges were found to be quite positive. All of these values were observed to undergo significant fluctuations in response to changes in molecular orientation, with the carbonyl carbon bearing the greatest changes. These rotational variances were found to be considerably smaller when points close to the molecule were omitted from the fit, as shown in Table II. For example, the standard deviation of the nitrogen charge (0.0085) is about half that of the corresponding value in Table I (0.0177).

The magnitudes of the calculated point charges were found to be somewhat dependent upon the choice of exclusion radii. When larger exclusion radii were used (Table II), the carbonyl carbon charge was calculated to be somewhat more positive (0.8930), and the oxygen charge more negative (−0.6000) than when smaller radii were used. It seems likely that, in this case, the fit is more weighted toward the oxygen charge, since there are fewer sampling points near the carbon atom.

The new CHELPG method was applied to the same set of structures used in the CHELP calculations using both sparse and dense point sampling. The data in Tables III and IV show that the orientation-related charge variations calculated by high-density CHELPG were an order of

Table I. CHELP charges (small radii) of formamide *syn* rotational transition state (6-31G**/6-31G*).

Orientation	N	C	O	H(ald)	Ha(NH_2)	Hb(NH_2)	Dipole	Points
Normal	−1.0703	0.9000	−0.5998	−0.0405	0.4053	0.4053	1.61005	388
30° (x)	−1.0943	0.9077	−0.6065	−0.0340	0.4126	0.4145	1.60124	391
30° (y)	−1.0907	0.8072	−0.5648	0.0025	0.4229	0.4229	1.54863	393
30° (z)	−1.1086	0.9430	−0.6211	−0.0475	0.4168	0.4174	1.62980	394
45° (x)	−1.0699	0.8639	−0.5847	−0.0245	0.4076	0.4076	1.56940	391
45° (y)	−1.0584	0.8509	−0.5793	−0.0237	0.4053	0.4053	1.58430	389
45° (z)	−1.0933	0.8967	−0.6028	−0.0293	0.4143	0.4143	1.59974	396
Average	−1.0836	0.8813	−0.5941	−0.0281	0.4131	0.4125	1.59188	
Std. Dev.	0.0177	0.0444	0.0190	0.0160	0.0087	0.0067	0.02693	

6-31G**/6-31G* Dipole Moment = 1.57330 Debye

Table Ia. CHELP charges (small radii) of formamide *syn* rotational transition state, dense sampling.

Orientation	N	C	O	H(ald)	Ha(NH_2)	Hb(NH_2)	Dipole	Points
Normal	−1.0645	0.9931	−0.6359	−0.0833	0.3953	0.3953	1.68739	3016
30° (x)	−1.0797	0.9545	−0.6200	−0.0619	0.4009	0.4063	1.62563	3031
30° (y)	−1.0766	0.8632	−0.5843	−0.0253	0.4115	0.4115	1.57855	3018
30° (z)	−1.0730	1.0003	−0.6412	−0.0815	0.3950	0.4004	1.69089	3064
45° (x)	−1.0612	0.8934	−0.5980	−0.0391	0.4025	0.4025	1.61922	3016
45° (y)	−1.0733	0.8824	−0.5914	−0.0352	0.4087	0.4087	1.59671	3001
45° (z)	−1.0751	0.9706	−0.6294	−0.0681	0.4010	0.4010	1.66516	3069
Average	−1.0719	0.9368	−0.6143	−0.0563	0.4021	0.4037	1.63765	
Std. Dev.	0.0066	0.0562	0.0229	0.0232	0.0062	0.0055	0.04419	

Table II. CHELP charges (large radii) of formamide *syn* rotational transition state (6-31G**/6-31G*).

Orientation	N	C	O	H(ald)	Ha(NH_2)	Hb(NH_2)	Dipole	Points
Normal	−1.0781	0.9156	−0.6100	−0.0430	0.4078	0.4078	1.64277	383
30° (*x*)	−1.1007	0.9071	−0.6063	−0.0315	0.4156	0.4157	1.58771	388
30° (*y*)	−1.0793	0.8577	−0.5851	−0.0191	0.4129	0.4129	1.58375	383
30° (*z*)	−1.0759	0.9516	−0.6209	−0.0622	0.4040	0.4033	1.65534	385
45° (*x*)	−1.0785	0.8658	−0.5891	−0.0205	0.4112	0.4112	1.58459	384
45° (*y*)	−1.0835	0.8491	−0.5818	−0.0141	0.4152	0.4152	1.57091	379
45° (*z*)	−1.0796	0.9042	−0.6068	−0.0372	0.4097	0.4097	1.64358	388
Average	−1.0822	0.8930	−0.6000	−0.0325	0.4109	0.4108	1.60981	
Std. Dev.	0.0085	0.0370	0.0147	0.0167	0.0042	0.0044	0.03563	

Table IIa. CHELP charges (large radii) of formamide *syn* rotational transition state, dense sampling.

Orientation	N	C	O	H(ald)	Ha(NH_2)	Hb(NH_2)	Dipole	Points
Normal	−1.0725	0.9406	−0.6164	−0.0570	0.4027	0.4027	1.64092	3081
30° (*x*)	−1.0799	0.9134	−0.6057	−0.0424	0.4073	0.4074	1.60430	3012
30° (*y*)	−1.0760	0.8388	−0.5790	−0.0105	0.4133	0.4133	1.57959	3004
30° (*z*)	−1.0783	0.9148	−0.6094	−0.0430	0.4075	0.4083	1.64030	3025
45° (*x*)	−1.0783	0.8758	−0.5915	−0.0272	0.4106	0.4106	1.58979	3083
45° (*y*)	−1.0758	0.8564	−0.5831	−0.0202	0.4113	0.4113	1.57446	3075
45° (*z*)	−1.0808	0.9157	−0.6106	−0.0414	0.4085	0.4085	1.63797	3032
Average	−1.0774	0.8936	−0.5994	−0.0345	0.4087	0.4089	1.60962	
Std. Dev.	0.0028	0.0371	0.0147	0.0159	0.0034	0.0034	0.02968	

Table III. CHELPG charges (small radii) of formamide *syn* rotational transition state (6-31G**/6-31G*).

Orientation	N	C	O	H(ald)	Ha(NH_2)	Hb(NH_2)	Dipole	Points
Normal	−1.0650	0.9482	−0.6164	−0.0628	0.3980	0.3980	1.62587	6007
30° (*x*)	−1.0626	0.9429	−0.6147	−0.0615	0.3978	0.3980	1.63099	5983
30° (*y*)	−1.0615	0.9479	−0.6168	−0.0636	0.3970	0.3970	1.63651	5978
30° (*z*)	−1.0638	0.9439	−0.6153	−0.0610	0.3979	0.3983	1.62898	5966
45° (*x*)	−1.0614	0.9397	−0.6133	−0.0602	0.3979	0.3974	1.62835	6000
45° (*y*)	−1.0625	0.9431	−0.6148	−0.0614	0.3978	0.3978	1.63109	5982
45° (*z*)	−1.0609	0.9418	−0.6143	−0.0610	0.3972	0.3972	1.63000	5980
Average	−1.0625	0.9439	−0.6151	−0.0616	0.3977	0.3977	1.63026	
Std. Dev.	0.0015	0.0031	0.0012	0.0012	0.0004	0.0005	0.00329	

Table IIIa. CHELPG charges (small radii) of formamide *syn* rotational transition state, sparse sampling.

Orientation	N	C	O	H(ald)	Ha(NH_2)	Hb(NH_2)	Dipole	Points
Normal	−1.0507	0.9216	−0.6036	−0.0566	0.3947	0.3947	1.60913	282
30° (*x*)	−1.0629	0.9453	−0.6127	−0.0644	0.3997	0.3951	1.61306	307
30° (*y*)	−1.0529	0.9034	−0.6027	−0.0439	0.3981	0.3981	1.63525	286
30° (*z*)	−1.0698	0.9479	−0.6143	−0.0634	0.4004	0.3992	1.60976	303
45° (*x*)	−1.0548	0.9449	−0.6141	−0.0653	0.3941	0.3952	1.63372	312
45° (*y*)	−1.0633	0.9176	−0.6085	−0.0479	0.4010	0.4010	1.63732	290
45° (*z*)	−1.0743	0.9621	−0.6197	−0.0681	0.4000	0.4000	1.60998	301
Average	−1.0612	0.9347	−0.6108	−0.0585	0.3983	0.3976	1.62121	
Std. Dev.	0.0089	0.0208	0.0062	0.0094	0.0028	0.0026	0.01343	

magnitude smaller than the variations observed in the CHELP results, while the sparse sampling CHELPG results still showed a significant improvement over the corresponding CHELP results. Charges obtained using CHELPG were found to be somewhat more dependent upon the size of the exclusion radii than CHELP charges, but it is difficult to make a valid comparison between these dependencies, since the CHELP data is considerably more scattered.

It is interesting to note that in the high-density CHELPG results, the symmetry-related hy-

Table IV. CHELPG charges (large radii) of formamide *syn* rotational transition state (6-31G**/6-31G*).

Orientation	N	C	O	H(ald)	Ha(NH_2)	Hb(NH_2)	Dipole	Points
Normal	−1.0674	0.8950	−0.5996	−0.0377	0.4049	0.4049	1.62018	5356
30° (*x*)	−1.0684	0.9013	−0.6014	−0.0403	0.4046	0.4043	1.61760	5353
30° (*y*)	−1.0644	0.8965	−0.5995	−0.0395	0.4034	0.4034	1.61949	5339
30° (*z*)	−1.0675	0.8998	−0.6011	−0.0398	0.4046	0.4040	1.61897	5328
45° (*x*)	−1.0691	0.8999	−0.6015	−0.0391	0.4050	0.4049	1.61990	5369
45° (*y*)	−1.0649	0.8954	−0.5994	−0.0384	0.4036	0.4036	1.61874	5354
45° (*z*)	−1.0659	0.9026	−0.6022	−0.0412	0.4033	0.4033	1.62256	5340
Average	−1.0668	0.8986	−0.6007	−0.0394	0.4042	0.4041	1.61963	
Std. Dev.	0.0018	0.0030	0.0015	0.0012	0.0007	0.0007	0.00155	

Table IVa. CHELPG charges (large radii) of formamide *syn* rotational transition state, sparse sampling.

Orientation	N	C	O	H(ald)	Ha(NH_2)	Hb(NH_2)	Dipole	Points
Normal	−1.0781	0.9344	−0.6116	−0.0534	0.4043	0.4043	1.60417	264
30° (*x*)	−1.0675	0.9164	−0.6047	−0.0481	0.4024	0.4014	1.60573	274
30° (*y*)	−1.0610	0.9226	−0.6086	−0.0530	0.4000	0.3999	1.63920	258
30° (*z*)	−1.0691	0.9133	−0.6049	−0.0459	0.4039	0.4026	1.61409	273
45° (*x*)	−1.0540	0.8909	−0.5957	−0.0419	0.3997	0.4011	1.62709	278
45° (*y*)	−1.0691	0.9093	−0.6035	−0.0438	0.4036	0.4036	1.61148	276
45° (*z*)	−1.0750	0.9311	−0.6132	−0.0516	0.4043	0.4043	1.63210	268
Average	−1.0677	0.9169	−0.6060	−0.0482	0.4026	0.4025	1.61912	
Std. Dev.	0.0081	0.0146	0.0058	0.0046	0.0020	0.0017	0.01373	

Table V. CHELP charges (small radii) of planar formamide (6-31G**/6-31G*).

Orientation	N	C	O	H(ald)	Ha(NH_2)	Hb(NH_2)	Dipole	Points
Normal	−1.0367	0.9232	−0.6732	−0.0655	0.4456	0.4056	4.15366	396
30° (*x*)	−1.0202	0.7600	−0.6090	−0.0013	0.4540	0.4164	4.10828	391
30° (*y*)	−1.0056	0.7607	−0.6039	−0.0098	0.4495	0.4091	4.05120	392
30° (*z*)	−1.0154	0.7780	−0.6135	−0.0150	0.4500	0.4159	4.11507	392
45° (*x*)	−1.0847	0.8198	−0.6259	−0.0144	0.4726	0.4325	4.08962	396
45° (*y*)	−1.0395	0.7841	−0.6132	−0.0097	0.4578	0.4205	4.07707	398
45° (*z*)	−1.0396	0.7890	−0.6140	−0.0160	0.4578	0.4229	4.09365	395
Average	−1.0345	0.8021	−0.6218	−0.0188	0.4553	0.4177	4.09836	
Std. Dev.	0.0258	0.0571	0.0236	0.0212	0.0088	0.0087	0.03218	

6-31G**/6-31G* Dipole Moment = 4.09460 Debye

Table Va. CHELP charges (small radii) of planar formamide (6-31G**/6-31G*), dense sampling.

Orientation	N	C	O	H(ald)	Ha(NH_2)	Hb(NH_2)	Dipole	Points
Normal	−1.0421	0.8726	−0.6453	−0.0534	0.4483	0.4199	4.12895	3071
30° (*x*)	−1.0124	0.8163	−0.6275	−0.0296	0.4425	0.4107	4.10341	3026
30° (*y*)	−1.0396	0.8258	−0.6272	−0.0314	0.4576	0.4149	4.06609	3039
30° (*z*)	−1.0386	0.8614	−0.6408	−0.0476	0.4474	0.4181	4.10984	3048
45° (*x*)	−1.0365	0.8608	−0.6407	−0.0452	0.4478	0.4137	4.08309	3063
45° (*y*)	−1.0370	0.7634	−0.6023	−0.0060	0.4569	0.4250	4.07393	3021
45° (*z*)	−1.0204	0.8379	−0.6330	−0.0404	0.4432	0.4127	4.09956	3045
Average	−1.0324	0.8340	−0.6310	−0.0362	0.4491	0.4164	4.09511	
Std. Dev.	0.0113	0.0373	0.0144	0.0158	0.0060	0.0049	0.0222	

drogens H_a and H_b are calculated to have the same atomic charge to within 0.0006, regardless of orientation, while the CHELP results show a larger violation of molecular symmetry (0.002). This apparent loss of symmetry is particularly large in cases where small exclusion radii are used (Table I). Other authors have observed this problem[8] and proposed that the molecule be manually aligned with one of the symmetry axes to prevent any distortion of symmetry-related multipoles. The simple solution cannot be in conformational analysis, where the charges calcu-

Table VI. CHELP charges (large radii) of planar formamide (6-31G**/6-31G*).

Orientation	N	C	O	H(ald)	Ha(NH_2)	Hb(NH_2)	Dipole	Points
Normal	−0.9706	0.7034	−0.5898	0.0118	0.4422	0.4030	4.09323	388
30° (*x*)	−1.0234	0.7587	−0.6060	−0.0013	0.4539	0.4181	4.09119	389
30° (*y*)	−1.0080	0.7367	−0.5987	0.0029	0.4558	0.4113	4.07741	380
30° (*z*)	−1.0459	0.8015	−0.6194	−0.0193	0.4580	0.4250	4.10757	387
45° (*x*)	−1.0463	0.7541	−0.6023	0.0038	0.4642	0.4267	4.08843	385
45° (*y*)	−0.9876	0.6685	−0.5737	0.0288	0.4499	0.4141	4.08300	380
45° (*z*)	−1.0630	0.8065	−0.6152	−0.0240	0.4622	0.4335	4.09068	387
Average	−1.0207	0.7471	−0.6007	0.0004	0.4552	0.4188	4.09022	
Std. Dev.	0.0338	0.0498	0.0155	0.0180	0.0075	0.0104	0.00940	

Table VIa. CHELP charges (large radii) of planar formamide (6-31G**/6-31G*), dense sampling.

Orientation	N	C	O	H(ald)	Ha(NH_2)	Hb(NH_2)	Dipole	Points
Normal	−1.0161	0.7581	−0.6048	−0.0073	0.4517	0.4184	4.10575	3053
30° (*x*)	−1.0066	0.7524	−0.6047	−0.0029	0.4477	0.4141	4.10136	3020
30° (*y*)	−1.0184	0.7315	−0.5962	0.0072	0.4583	0.4175	4.08740	3029
30° (*z*)	−1.0104	0.7599	−0.6067	−0.0075	0.4484	0.4162	4.10995	3035
45° (*x*)	−1.0578	0.7579	−0.6017	0.0003	0.4675	0.4321	4.08722	3003
45° (*y*)	−1.0167	0.6975	−0.5814	0.0201	0.4568	0.4237	4.08728	3009
45° (*z*)	−1.0051	0.7598	−0.6071	−0.0082	0.4466	0.4139	4.10726	3042
Average	−1.0187	0.7456	−0.6004	−0.0002	0.4538	0.4194	4.09803	
Std. Dev.	0.0180	0.0235	0.0092	0.0103	0.0075	0.0065	0.01036	

Table VII. CHELPG charges (small radii) of planar formamide (6-31G**/6-31G*).

Orientation	N	C	O	H(ald)	Ha(NH_2)	Hb(NH_2)	Dipole	Points
Normal	−0.9896	0.7934	−0.6191	−0.0247	0.4357	0.4043	4.08971	5940
30° (*x*)	−0.9926	0.8032	−0.6226	−0.0282	0.4356	0.4047	4.09165	5977
30° (*y*)	−0.9879	0.7900	−0.6184	−0.0229	0.4354	0.4038	4.09117	5939
30° (*z*)	−0.9962	0.8004	−0.6213	−0.0265	0.4375	0.4061	4.09112	5973
45° (*x*)	−0.9919	0.7964	−0.6205	−0.0251	0.4363	0.4048	4.09234	5959
45° (*y*)	−0.9891	0.7909	−0.6189	−0.0229	0.4361	0.4039	4.09162	5941
45° (*z*)	−0.9964	0.8045	−0.6225	−0.0284	0.4369	0.4059	4.08905	5966
Average	−0.9920	0.7970	−0.6205	−0.0255	0.4362	0.4048	4.09095	
Std. Dev.	0.0034	0.0059	0.0017	0.0023	0.0008	0.0009	0.00116	

Table VIIa. CHELPG charges (small radii) of planar formamide (6-31G**/6-31G*), sparse sampling.

Orientation	N	C	O	H(ald)	Ha(NH_2)	Hb(NH_2)	Dipole	Points
Normal	−0.9778	0.7427	−0.6025	−0.0071	0.4367	0.4081	4.12376	280
30° (*x*)	−0.9944	0.8118	−0.6258	−0.0294	0.4362	0.4017	4.07253	319
30° (*y*)	−0.9832	0.7619	−0.6072	−0.0153	0.4364	0.4065	4.09907	300
30° (*z*)	−1.0201	0.8365	−0.6304	−0.0408	0.4417	0.4131	4.08370	291
45° (*x*)	−0.9970	0.8002	−0.6206	−0.0273	0.4374	0.4076	4.09449	305
45° (*y*)	−0.9810	0.7447	−0.6026	−0.0066	0.4370	0.4086	4.11550	284
45° (*z*)	−1.0180	0.8097	−0.6205	−0.0310	0.4430	0.4168	4.09531	298
Average	−0.9958	0.7868	−0.6157	−0.0225	0.4383	0.4089	4.09780	
Std. Dev.	0.0174	0.0368	0.0114	0.0130	0.0028	0.0078	0.01750	

lated for symmetric structures are to be compared with non-symmetric ones.

CHELP and CHELPG results for planar structure **1** are presented in Tables V–VIII. Again, the CHELPG results were found to be much less sensitive towards molecular orientation than the CHELP results proved to be. For example, the standard deviation of the high-density CHELPG carbonyl carbon charges for multiple orientations of **1** is only 0.0059 when computed using the "small" exclusion radii (Table VII), and 0.0030 using the "large" radii (Table VIII). The corresponding high-density CHELP standard deviations are 0.0373 (Table Va) and 0.0235

Table VIII. CHELPG charges (large radii) of planar formamide (6-31G**/6-31G*).

Orientation	N	C	O	H(ald)	Ha(NH_2)	Hb(NH_2)	Dipole	Points
Normal	−0.9858	0.7288	−0.5969	0.0029	0.4416	0.4094	4.10042	5327
30° (*x*)	−0.9856	0.7283	−0.5966	0.0028	0.4415	0.4096	4.10127	5328
30° (*y*)	−0.9849	0.7293	−0.5972	0.0025	0.4412	0.4090	4.10095	5303
30° (*z*)	−0.9830	0.7249	−0.5955	0.0040	0.4408	0.4088	4.10084	5346
45° (*x*)	−0.9872	0.7302	−0.5972	0.0022	0.4419	0.4100	4.10188	5339
45° (*y*)	−0.9884	0.7330	−0.5981	0.0013	0.4420	0.4101	4.10111	5304
45° (*z*)	−0.9843	0.7246	−0.5954	0.0043	0.4413	0.4094	4.10162	5329
Average	−0.9856	0.7284	−0.5967	0.0029	0.4415	0.4095	4.10116	
Std. Dev.	0.0018	0.0030	0.0010	0.0010	0.0004	0.0005	0.00049	

Table VIIIa. CHELPG charges (large radii) of planar formamide (6-31G**/6-31G*), sparse sampling.

Orientation	N	C	O	H(ald)	Ha(NH_2)	Hb(NH_2)	Dipole	Points
Normal	−1.0106	0.7670	−0.6078	−0.0103	0.4466	0.4152	4.09319	260
30° (*x*)	−0.9896	0.7330	−0.5952	−0.0006	0.4409	0.4115	4.08455	289
30° (*y*)	−1.0078	0.7600	−0.6053	−0.0084	0.4439	0.4175	4.10738	274
30° (*z*)	−0.9783	0.7335	−0.5991	0.0004	0.4378	0.4058	4.09713	256
45° (*x*)	−0.9930	0.7443	−0.6015	−0.0038	0.4429	0.4110	4.10141	277
45° (*y*)	−0.9960	0.7596	−0.6075	−0.0089	0.4426	0.4102	4.10188	272
45° (*z*)	−0.9378	0.7054	−0.5944	0.0075	0.4279	0.3914	4.10623	264
Average	−0.9876	0.7433	−0.6015	−0.0034	0.4404	0.4089	4.09880	
Std. Dev.	0.0245	0.0214	0.0056	0.0064	0.0061	0.0086	0.00800	

(Table VIa), respectively. The low-density CHELP G data are 0.0368 (Table VIIa) and 0.0214 (Table VIIIa), while the normal CHELP results are 0.0571 (Table V) and 0.0498 (Table VI). This trend is also reflected in the other data in Tables 5–8. As in the case of the transition structure **2**, larger atomic exclusion radii cause the carbon atom to appear less positive and the oxygen atom to appear less negative than when smaller radii were used. This dependency of the point charge model on the particular exclusion radii chosen does not present a problem in practice; it merely serves to remind us that these "atomic charges" are really quite artificial. For most purposes, the actual values of the point charges are not terribly important; consistency and rotational invariance are of much greater concern.

In the second part of the investigation, charge variations along the C-N bond rotational pathway of formamide were examined. The geometries used in this study were obtained by performing a mode-walk calculation along the imaginary mode leading from transition state **2** to planar structure **1**.[12] The mode-walk was done in 33 steps at the 6-31G* level, with complete analytical forces computed at each point.[13] Details of this reaction-path following procedure will be published elsewhere. A selection of 11 points along the computed path were used in the 6-31G** single-point calculations.

The rotational pathway defined by the mode-walk consisted of an interesting set of deformations of the amino group coupled with the rotation. During the initial part of the walk, the pyramidal amino group rotated as a unit until just after hydrogen H_a had eclipsed the carbonyl group. After a slight overshoot, hydrogen H_a relaxed back to a position *syn* to the carbonyl oxygen, while H_b continued rotation until it had arrived at this final *anti* position. Curiously, the total energy of the system was found to be within

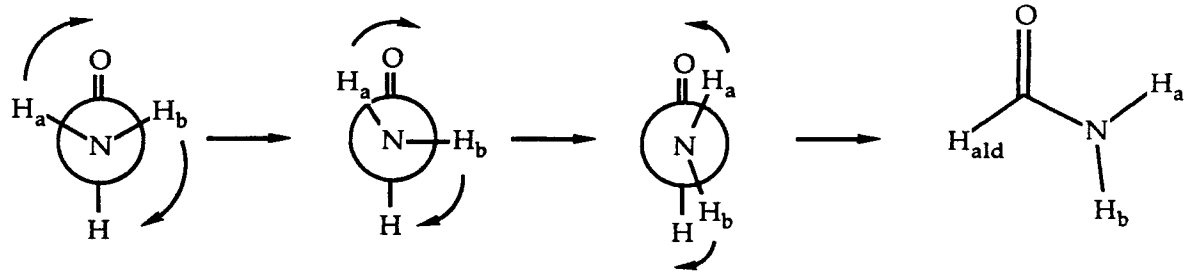

2 **1**

1.5 kcal/mole of the ground-state energy as soon as hydrogen H_a had begun to relax toward the carbonyl oxygen. This is consistent with experimental IR data which suggests that the NH_2 "wagging" mode has a soft harmonic potential (ca. 110 cm^{-1}) together with a rather steep quartic component.[14]

As a result of using a mode-walk pathway as the rotational "reaction coordinate," no single geometric parameter could be used to define the progress of the rotation. Consequently, an independent variable had to be found which was related only to the degree of conversion from transition structure **2** to the planar minimum **1**. One solution to this problem was to use the position of the electrostatically determined nitrogen "lone pair" to define the rotation. Therefore, a "lone pair" vector was defined by subtracting the nitrogen nuclear coordinates from the position of the electrostatic potential minimum in the vicinity of the nitrogen atom.[15] This definition is quite general, since it can accommodate complex atomic motions along the reaction coordinate, and does not rely on any arbitrary reference plane. The values of the electrostatic potential minima for each of the intermediate structures are shown in Figure 5, plotted against the dihedral angle that the "lone-pair" vector makes with the carbonyl group. It is significant that the

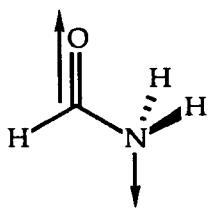

value of the electrostatic potential minimum decreases smoothly from about −10 kcal/mole in the planar structure **1** to −60 kcal/mole as the geometry approaches transition state **2**. This result agrees with vibrational and reactivity data which suggests that rotationally-deformed amides should behave more like amino-ketones. The potential minimum did not reach a value near the −82.5 kcal/mol calculated for the amino-group of staggered methylamine, but that is presumably due to the electron withdrawing effect of the neighboring carbonyl group.

ELECTRONIC CHANGES IN FORMAMIDE UPON C-N BOND ROTATION

Amino Group Charge

Table IV shows the CHELPG (large radii) point-charge model of formamide undergoing changes due to rotation about the C-N bond from the planar minimum **1** to the *syn* rotational transition state **2**. The column marked Lp-N-C-O indicates the dihedral angle that the "lone pair" vector makes with respect to the carbonyl group. At the top of Table IX, the structure is in its planar form, where the "lone pair" direction is somewhat less than 90° from the carbonyl bond. As the rotation progresses, this angle increases to 180°. Table X shows the analogous CHELP results. Figure 1 depicts the changes which occur in the amino group along the pathway leading from the planar structure **1** to the transition state **2**, using the "lone pair" vector defined above as the independent variable. The heavy line indicates the high-density CHELPG monopole variations, while the lighter line indicates the CHELP results. On the left side of the graph, the molecule is in its planar form **1**, with the lone-pair vector pointed nearly perpendicular to the molecular plane. Continuing across the graph, the lone-pair vector moves in concert with the amino group rotation until it is directed *anti* to the carbonyl C-O bond at the *syn* rotational transition state **2**. Since the overall changes in monopole charge are fairly large for this group, both CHELP and CHELPG give similar qualitative results, but the CHELPG changes are sig-

Table IX. CHELPG charges (large radii) of formamide during rotation from planar to *syn* rotational transition state (6-31G**/6-31G*), standard orientation geometries.

Lp-N-C-O	N	C	O	H(ald)	Ha(NH_2)	Hb(NH_2)
86.8°	−0.9843	0.7277	−0.5970	0.0035	0.4414	0.4087
87.1°	−0.9833	0.7267	−0.5970	0.0035	0.4414	0.4087
87.3°	−0.9623	0.7117	−0.5920	0.0075	0.4344	0.4007
95.8°	−0.9293	0.7007	−0.5840	0.0095	0.4154	0.3877
106.9°	−0.9463	0.7287	−0.5850	0.0035	0.4134	0.3857
118.7°	−0.9693	0.7667	−0.5890	−0.0055	0.4104	0.3867
130.6°	−0.9953	0.8027	−0.5910	−0.0135	0.4084	0.3887
142.7°	−1.0243	0.8427	−0.5950	−0.0245	0.4074	0.3927
155.0°	−1.0483	0.8757	−0.6010	−0.0325	0.4084	0.3967
167.6°	−1.0613	0.8947	−0.6020	−0.0385	0.4064	0.3997
180.0°	−1.0673	0.8937	−0.5990	−0.0365	0.4044	0.4047

Table X. CHELP charges (small radii) of formamide during rotation from planar to *syn* rotational transition state (6-31G**/6-31G*), standard orientation geometries.

Lp-N-C-O	N	C	O	H(ald)	Ha(NH_2)	Hb(NH_2)
86.8°	−1.0364	0.8021	−0.6163	−0.0118	0.4559	0.4185
87.1°	−0.9844	0.7801	−0.6123	−0.0118	0.4429	0.3985
87.3°	−1.0194	0.8641	−0.6363	−0.0448	0.4419	0.4075
95.8°	−1.0004	0.8281	−0.6213	−0.0278	0.4339	0.3985
106.9°	−0.9714	0.7651	−0.5953	0.0012	0.4269	0.3855
118.7°	−1.0024	0.8661	−0.6183	−0.0348	0.4159	0.3855
130.6°	−1.0114	0.8591	−0.6283	−0.0308	0.4119	0.3865
142.7°	−1.0164	0.8651	−0.6373	−0.0318	0.4049	0.3855
155.0°	−1.0524	0.9151	−0.6083	−0.0438	0.4099	0.3925
167.6°	−1.0784	0.9401	−0.6123	−0.0498	0.4119	0.4015
180.0°	−1.0574	0.8611	−0.5783	−0.0238	0.4049	0.4055

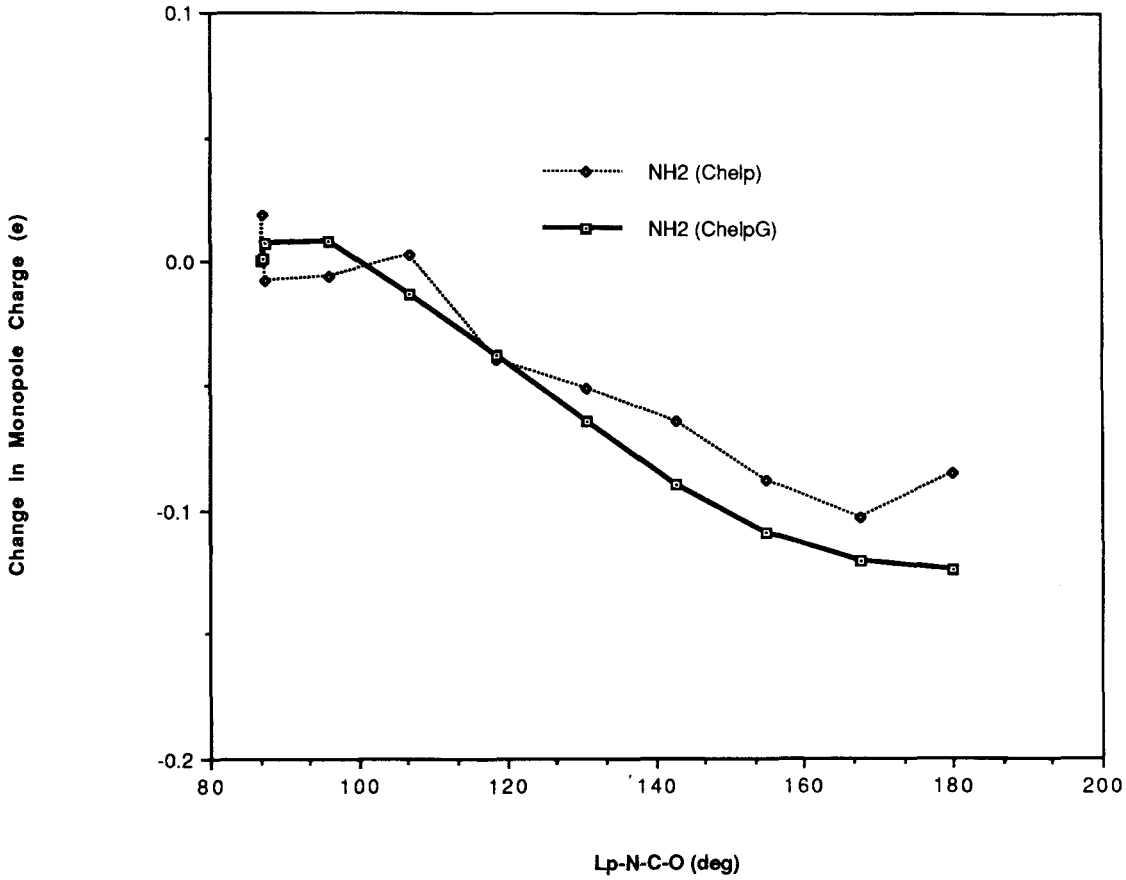

Figure 1. Amino group.

nificantly smoother. As expected from simple electrostatic potential considerations, the total charge on the amino group is less negative in planar conformation **1** than in transition structure **2**. This is in marked contrast to the results obtained by Wiberg and Laidig[16] using Bader's theory of atoms in molecules.[4] In that investigation, it was noted that the amino group has a higher electron population in the planar form than in either rotational transition state, and that the additional charge density comes from further depletion of the carbonyl carbon population. This apparent disparity is a result of the fact that the PROAIMS technique provides atomic information from an intramolecular perspective, while electrostatic potential-derived charges simply provide a convenient external view of the charge density distribution. As with any atom-centered monopole model, the CHELPG charges refer to spherically symmetric atoms, whereas the atoms defined by PROAIMS are markedly anisotropic. A detailed comparison of the results of these two methods is in preparation.

Carbonyl Carbon Charge

The changes which occur in the potential-derived carbonyl charge are shown in Figure 2. Large differences between the CHELP and CHELPG values are seen throughout the rotation. This is

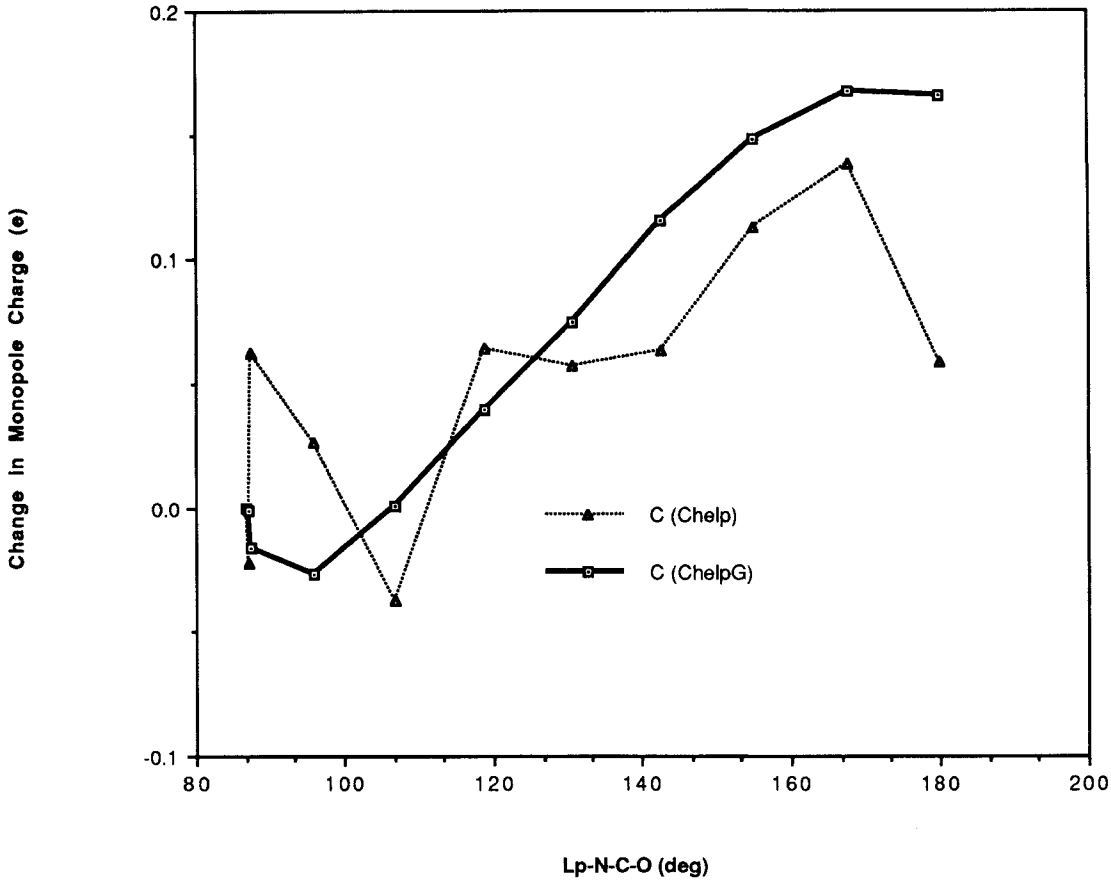

Figure 2. Carbonyl carbon.

mostly likely a result of the sparse sampling in the neighborhood of the carbonyl carbon in the CHELP treatment. It is significant that the change in the carbonyl carbon charge calculated by CHELPG is nearly equal and opposite to the amino group total charge variation.

Carbonyl Oxygen Charge

As shown in Figure 3, the carbonyl oxygen charge is relatively unchanged throughout the rotation. This data corroborates other results which suggest that the C-N rotational barrier in amides does not arise from the traditional charge delocalization model shown below, but is instead due to an exchange of electron density and its associated kinetic energy between the amino nitrogen and the carbonyl carbon.[17]

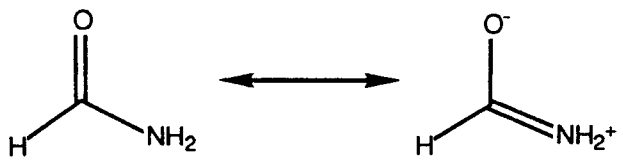

Aldehyde Hydrogen Charge

Figure 4 illustrates the changes which occur in the aldehyde hydrogen point charge upon C-N bond rotation. The changes are rather small compared to the amino group and carbonyl carbon charge variations, but once again, the CHELPG procedure gives a smooth curve, while the CHELP results are quite scattered.

CONCLUSIONS

In order to achieve a reasonable level of rotational invariance in potential-derived point charges, a large number of regularly spaced points must be used in the fitting procedure. This requirement was found to be especially important in conformational studies. The CHELP and CHELPG potential-derived charges were found to be relatively insensitive to the size of the exclusion radii, provided that enough points are sampled near each monopole site. The described CHELPG high density sampling technique allows such conformational studies as demonstrated by the analysis of the formamide molecule during C-N bond rotation.

The results presented for C-N bond rotation in formamide suggest that from an external point of view, the amino nitrogen in the planar form (**1**) appears less negative than in the pyramidal *syn* transition structure (**2**). This result is in agreement with some of the established properties of planar and rotationally deformed

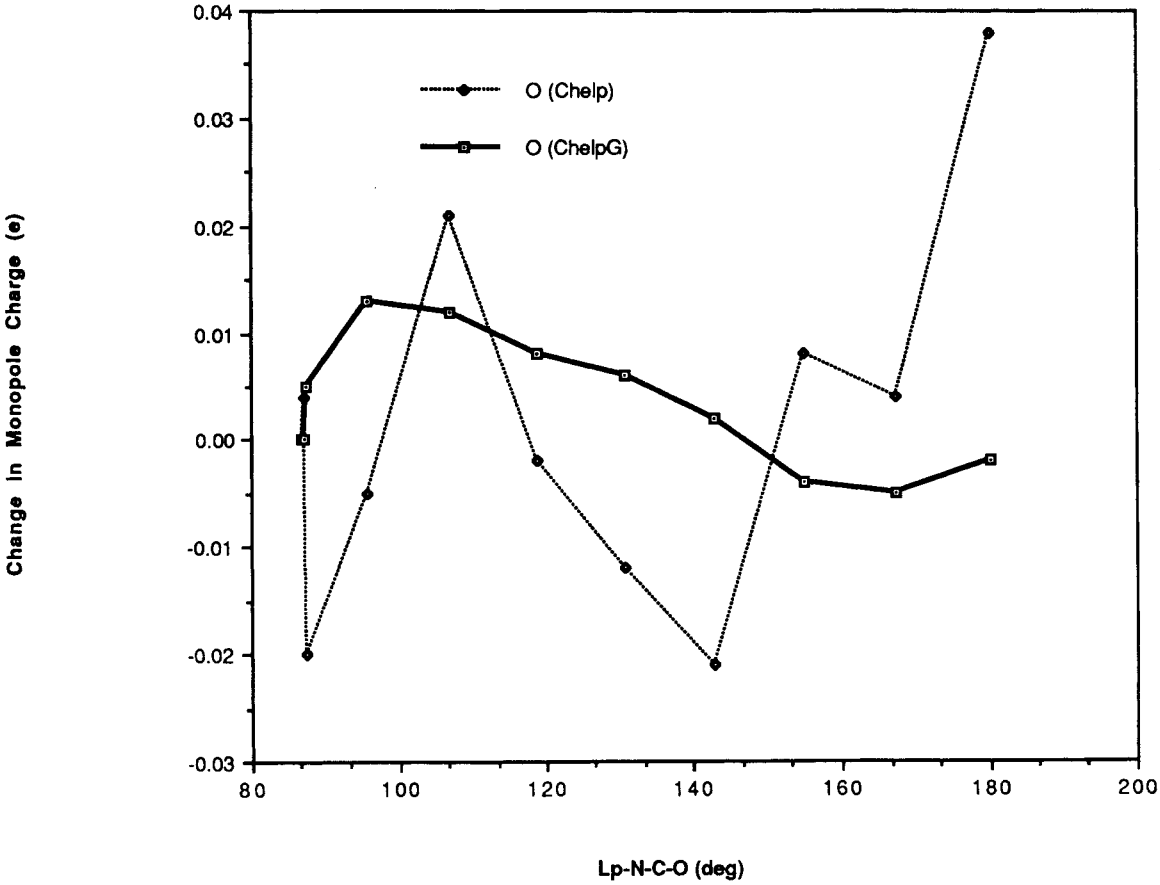

Figure 3. Carbonyl oxygen.

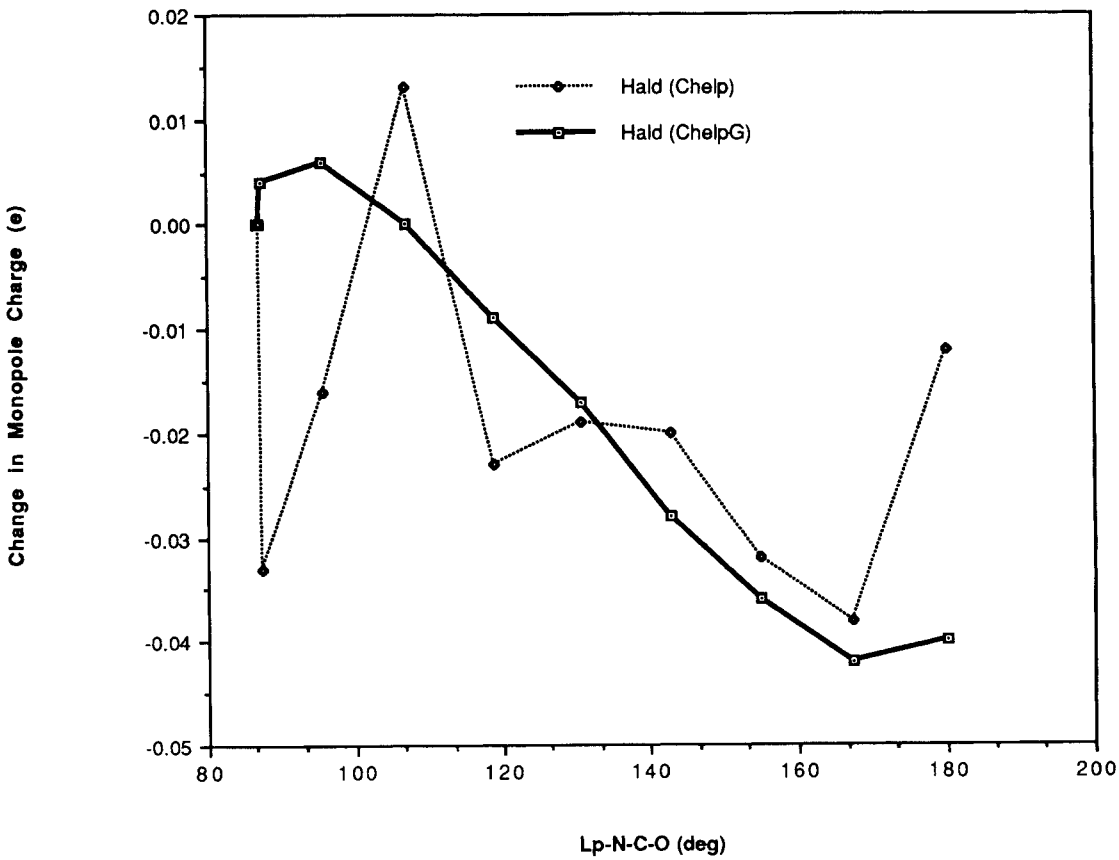

Figure 4. Aldehyde hydrogen.

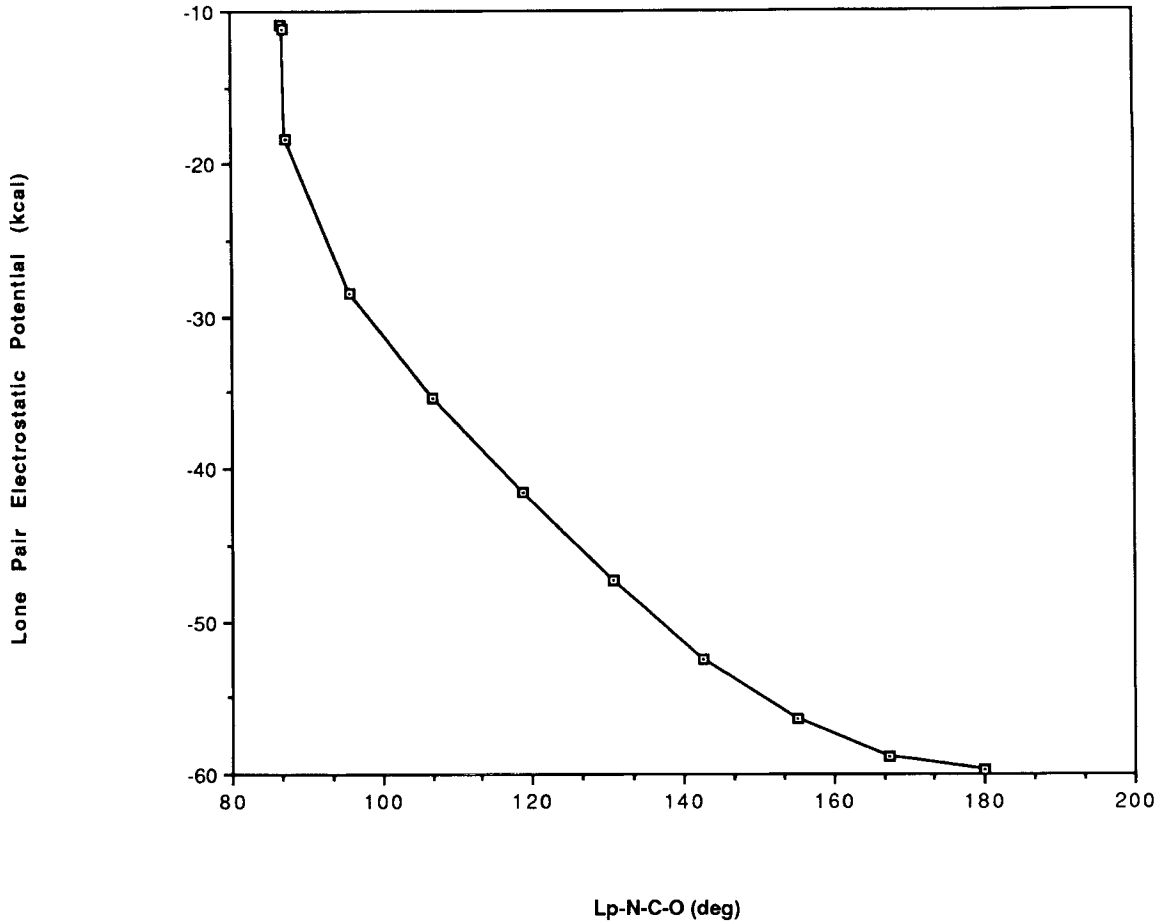

Figure 5. "Lone pair" electrostatic potential minima.

amides.[18] The lack of change of the carbonyl oxygen monopole upon rotation, however, is contrary to the widely accepted explanation for amide resonance, but agrees with the recent explanation of amide stabilization put forth by Wiberg and Laidig.[14]

CALCULATIONAL METHODS

The *ab-initio* calculations reported in this article were performed on Multiflow Trace 7/200 and Trace 14/300 minisupercomputers using both the public Gaussian 86 program[19] and a developmental version of the Gaussian 88/90 program.[20] The rotational mode-walking calculations were accomplished using an eigenvector following algorithm implemented in the developmental Gaussian 88/90 program. The CHELP and CHELPG calculations were performed on a Trace 7/200 minisupercomputer and several Microvax II computers. Typical calculation times for the low-density (250-400 points) CHELP and CHELPG runs were 65-90 seconds on the Trace-7/200 (12-20 minutes on a Microvax II), while the high-density (3000-6000 points) CHELP and CHELPG runs required 18–35 minutes on the Trace 7/200.

This investigation was supported by a grant from the National Institutes of Health. The Trace 7/200 computer was obtained with the aid of an NIH instrument grant.

References

1. L. E. Chirlian and M. M. Francl, *J. Comp. Chem.*, **8,** 894 (1987).
2. For a review, see E. Scrocco and J. Tomasi, *Adv. Quantum Chem.*, **11,** 115, (1978).
3. For example, the AMBER force-field uses a point-charge approximation of electrostatic interactions. See: P. K. Wiener and P. A. Kollman, *J. Comp. Chem.*, **2,** 287 (1981).
4. F. W. Biegler-Konig, R. F. W. Bader, and T.-H. Tang, *J. Comp. Chem.*, **3,** 317 (1982). R. F. W. Bader, T.-H. Tang, Y. Tal, and F. W. Biegler-Konig, *J. Am. Chem. Soc.*, **104,** 946 (1982).
5. F. A. Momany, *J. Phys. Chem.*, **82,** 592 (1978).
6. P. H. Smit, J. L. Derissen, and F. B. van Duijneveldt, *Mol. Phys.*, **37,** 521 (1979).
7. U. C. Singh and P. A. Kollman, *J. Comp. Chem.*, **1984,** 5, 129.
8. The PDM88 program (QCPE) can fit an atom (and bond)-centered multipole series to the molecular electrostatic potential. See: D. E. Williams, *J. Comp. Chem.*, **9,** 745, (1988).
9. S. R. Cox and D. E. Williams, *J. Comp. Chem.*, **2,** 304 (1981).
10. M. Connolly, *QCPE* Program 429 (1982).
11. The sizes of the "small" exclusion radii were selected on the basis of electron density consider-

ations, using the standard values in reference 1 as a guide. The "large" radii were chosen as an arbitrary distance that would always be outside of regions where local changes in electrostatic potential are large.
12. The results in Table IX and Figures 1–4 are presented in the reverse order for clarity.
13. The mode-walking was done using the EF mode-walk algorithm incorporated in Gaussian90.
14. E. Hirota, R. Sugisaki, C.J. Nielsen, and G.O. Sorensen, *J. Mol. Spectrosc.*, **49,** 251 (1974).
15. The electrostatic potential minima were located using the automated search procedure in Gaussian88/90.
16. K.B. Wiberg and K.E. Laidig, *J. Am. Chem. Soc.*, **109,** 5935, (1987).
17. C.M. Breneman and K.B. Wiberg, manuscript in preparation.
18. A. Greenberg, in "Structure and Reactivity" J.F. Liebman and A. Greenberg, Eds, VCH Publishers: Deerfield Beach, FL, 1987, Chapter 4.
19. M.J. Frisch, J.S. Binkley, H.B. Schlegel, K. Raghavachari, C.F. Melius, R.L. Martin, J.J.P. Stewart, F.W. Bobrowitcz, C.M. Rohlfing, L.R. Kahn, D.J. DeFrees, R. Seeger, R.A. Whiteside, D.J. Fox, E.M. Fleuder, and J.A. Pople, *Gaussian86,* Carnegie-Mellon Quantum Chemistry Publishing Unit, Pittsburgh, PA, 1984.
20. M.J. Frisch, M. Head-Gordon, H.B. Schlegel, K. Raghavachari, J.S. Binkely, C. Gonzalez, D.J. DeFrees, D.J. Fox, R.A. Whiteside, R. Seeger, C.F. Melius, J. Baker, R.L. Martin, L.R. Kahn, J.J.P. Stewart, E.M. Fleuder, S. Topiol, and J.A. Pople, *Gaussian90,* Developmental version, revision A, Gaussian, Inc., Pittsburgh, PA, 1988.